Ideas and perspectives: Synergies from co-deployment of negative emission technologies

Thorben Amann & Jens Hartmann

Supplementary material

S1. Development of global potassium/potash resources

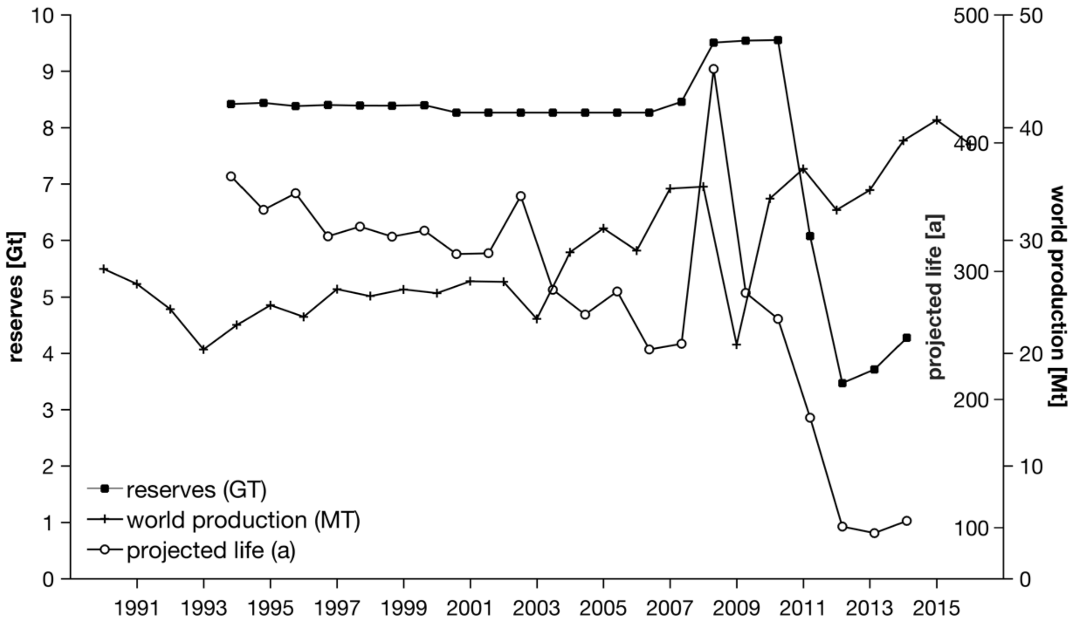

Fig. S 1-1 Update of data from Manning (2015), extended by the two most recent years. Data from Jasinski (2017), accessed through https://minerals.usgs.gov/minerals/pubs/commodity/potash/ on 2017-06-13.

S2. The underlying database *GEOROC*

The GEOROC data was downloaded from http://georoc.mpch-mainz.gwdg.de/georoc/, accessed on 2017-06-07. Data for volcanic rocks were downloaded as pre-compiled files. Only data for “type of material” = “Whole rock” and “Land/sea sampling” = “subaerial” were taken into consideration.

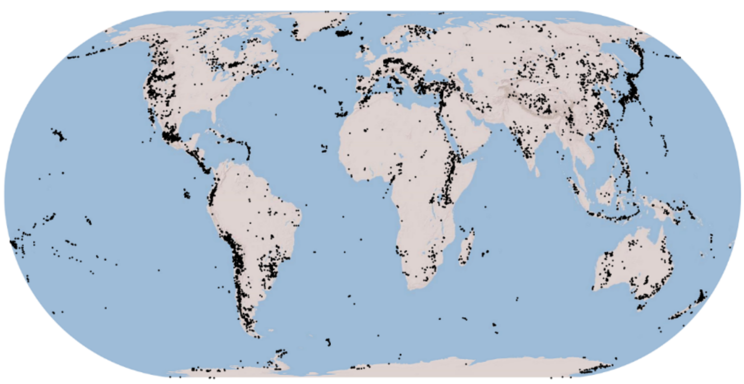

Fig. S 2-1 Global distribution of qualified samples in the GEOROC database.

S3. CO_2 capture potential

The ability to sequester atmospheric CO_2 is rock specific and depends on the cations that can be released during hydrolysis. It is defined as the carbon dioxide removal R_{CO2} in tonnes CO_2 per tonne of rock:

$$R_{CO_2} = \frac{M_{CO_2} * \sum(2n_{Ca^{2+}}, 2n_{Mg^{2+}}, n_{K^+}, n_{Na^+})}{1000} * \omega \qquad \text{Eq. S3-1}$$

n = molar amount of cation x, M_{CO2} = molar mass of CO_2, and ω = 0.85, factoring in seawater equilibration processes (cf. Fig. 1 in Renforth et al., 2013). They considered only divalent cations, where two charges bind about 1.7 moles CO_2 (~15% less, thus factor 0.85). Fig. 2 in the main paper shows only selected rock types. Fig. S3-1 provides an overview over R_{CO2} values of all volcanic rock types differentiated in the GEOROC database.

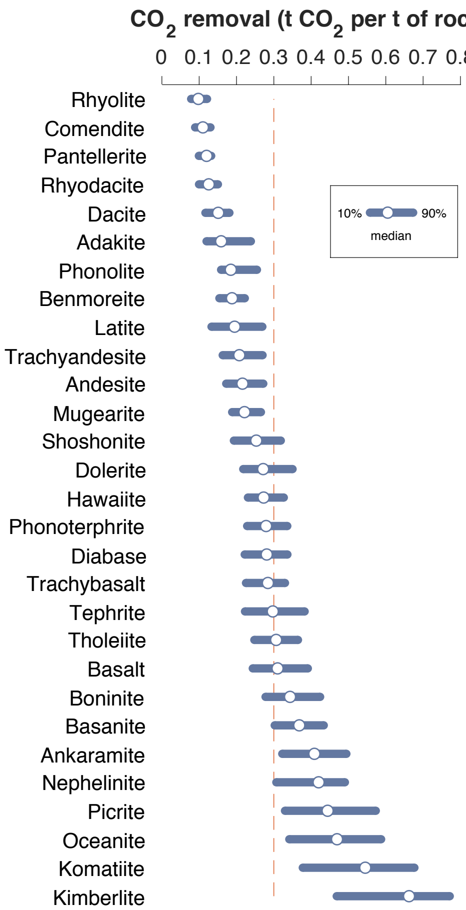

Fig. S 3-1 Calculated efficiency of CO_2 removal (R_{CO2}) for all rock types given in the GEOROC database. The dashed line is the pessimistic CO_2 emission during production of rock flour from Moosdorf et al. (2014).

S4. Calculation of element release rates

To compare potential element release differences between rock classes based on their relative rate of weathering and the relative composition of rock geochemistry, bulk weathering rates for a well-studied humid subtropical region (the Japanese Archipelago) comparable to areas of likely application are chosen (Hartmann and Moosdorf, 2011;Hartmann et al., 2013). The Japanese Archipelago is in general characterized by high weathering capacity in comparison to areas with depleted weathering profiles, where rates decrease by about 90% (Hartmann et al., 2014). For catchments that were dominated by basic and intermediate volcanic rocks, a weathering rate of 33 t base cations + Si km^{-2} a^{-1} was observed based on the analysis of nearly 400 catchments (Hartmann and Moosdorf, 2011). Field experiments with direct measurements of enhanced weathering rates due to finely ground rock product application, which would allow a more precise upscaling are still missing. The highest observed weathering rates of volcanic rocks including large areas of pyroclastics (comparable in some sense with EW) are about 3.5 times higher than rates calculated from Japanese catchments (Schopka et al., 2011). However, the temperature effect makes up for a about factor of two alone if the temperature difference between Japan and the Philippines are considered. Data from the latter study consider also the significant contribution of waters with higher residence time than expected in top soil treated by rock powder, which affects the overall dissolution rate of total rock compartment including the soils (Maher, 2011).

The P and K release rate by enhanced chemical weathering is calculated assuming that P and K are released at the same relative rate as major cations and silicon are released via weathering, as a first order estimate (Hartmann and Moosdorf, 2011) for each considered rock type and its reported geochemical composition using the data from the GEOROC database (Suppl. S1). As P and K are preferentially taken up by the ecosystems the calculations are considered to be conservative.

The first order upper boundary element release rate is calculated based on the major cation and silicon release rate and proportional to the total rock mass and assuming full dissolution as:

$$\frac{W_R}{\sum(\%Cations)_{sample}} \times c_{element} = element\ release\ rate\ [t\ km^{-2} a^{-1}] \qquad \textit{Eq. S4-1}$$

With W_R as the spatially explicit weathering rate (here 33 t base cations and Si km^{-2} a^{-1}) and *%Cations* as the rock specific values. This approach is suitable for geogenic nutrients like P and K. Elemental solubility, pH and redox processes directly affect the release and retention of trace metals like Cr or Ni, which is discussed separately.

S5. Nutrient removal by crop plants

In addition to the data for Miscanthus shown in the main text, we provide here additional data on crop plants that would potentially benefit from rock released nutrients (Fig. S5-1). The historical development of crop yields shows that the nutrient extraction of major crops increased steeply in the past (Fig. S5-2), indicating the need for a sustainable long-term nutrient cycle management, not only for new energy plants.

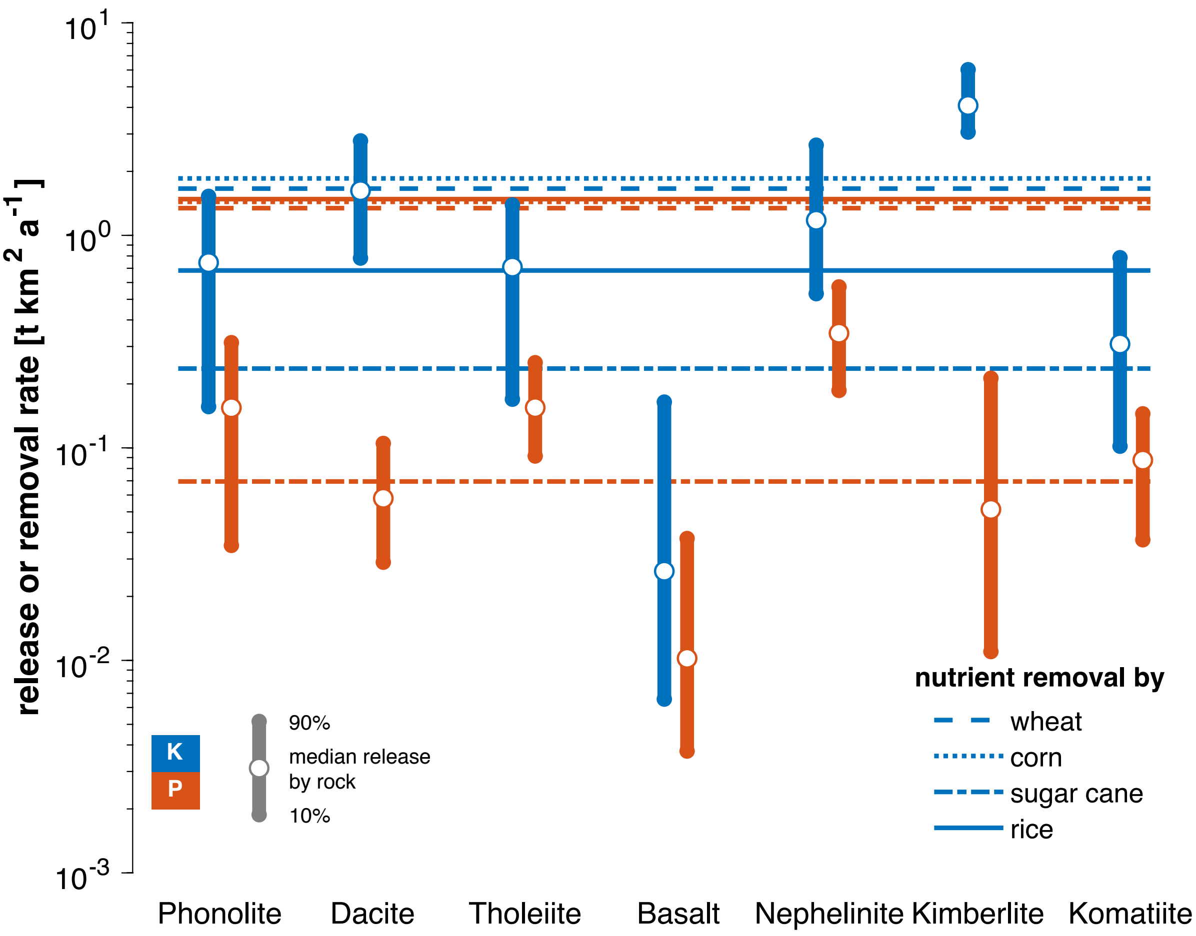

Fig. S5-1 Weathering release rates (circles; bars as variability indicator) of P and K from selected rocks (assuming their full dissolution during a natural weathering scenario based on subtropical Japanese catchments (cf. S4)) in comparison with the nutrient removal by harvesting the crops (dashed lines), i.e. the actual nutrient removal from the cropland, whereas residues are considered to remain on the land.

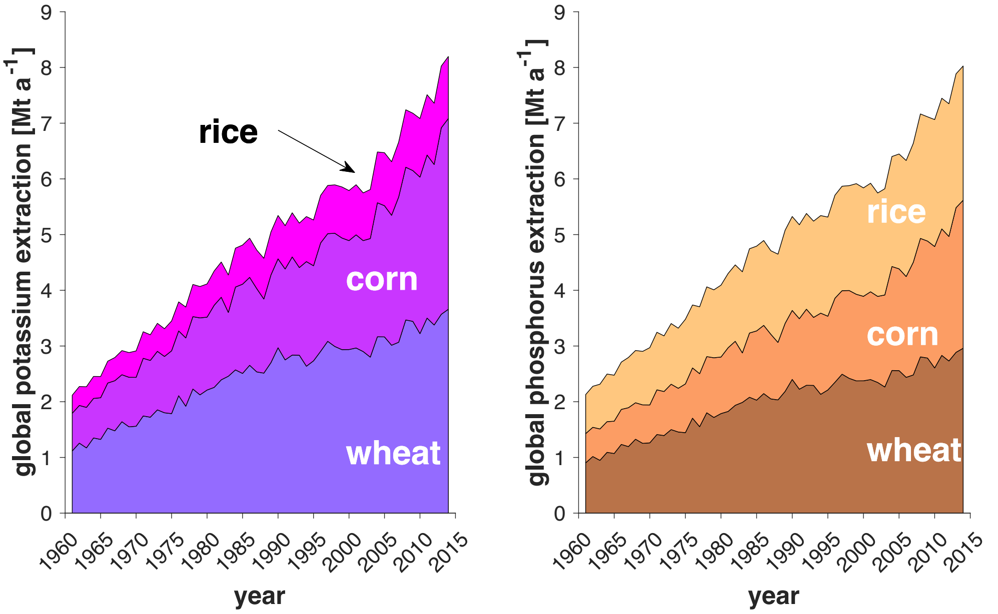

Fig. S5-2 The total annual global removal of K and P by harvest for three major crops over time. Data taken from FAOSTAT (2017).

The removal by nutrients was calculated based published data on crop yields (Tab. S5-1) and average contents of P and K from the literature in selected crop types (Tab. S5-2), considering only the harvestable material (mainly grains, for sugar cane: stalks, for Miscanthus: all harvestable parts):

$$Nutrient\ removal = \frac{Element\ content\ (\%)}{100} \times Yield \qquad \text{Eq. S5-1}$$

Tab. S5-1 Global average yields of selected crop plants.

Plant	Yield in 2014 (t km^{-2})	Reference
Barley	292.33	FAOSTAT (2017)
Corn	561.57	FAOSTAT (2017)
Rice	455.69	FAOSTAT (2017)
Soy beans	260.76	FAOSTAT (2017)
Sugar cane	6946.6	FAOSTAT (2017)
Wheat	330.74	FAOSTAT (2017)
	Observed yield min/max (t km^{-2})	
Miscanthus	40/4400	Brosse et al. (2012)

Tab. S5-2 Potassium and phosphorus contents in harvestable parts of plants (grains, stalks), in case of Miscanthus, the value refers to all harvestable parts.

Plant	K (% of biomass)	P (% of biomass)	Reference
Barley	0.009	0.01	Erbs et al. (2010)
Corn	0.33	0.256	Belitz (2009)
Rice	0.15	0.325	Belitz (2009)
Soy beans	2.05	0.67	Batal et al. (2010)
Sugar cane	0.0034	0.001	Fageria (1991)
Wheat	0.502	0.406	Belitz (2009)
Miscanthus min	0.11	0.04	Brosse et al. (2012)
Miscanthus max	1.58	0.11	Brosse et al. (2012)

References

Batal, A. B., Dale, N. M., and Saha, U. K.: Mineral composition of corn and soybean meal, The Journal of Applied Poultry Research, 19, 361-364, 10.3382/japr.2010-00206, 2010.

Belitz, H.-D.: Food chemistry, Fourth ed., edited by: Grosch, W., and Schieberle, P., Springer, Berlin u.a., 2009.

Brosse, N., Dufour, A., Meng, X., Sun, Q., and Ragauskas, A.: Miscanthus: a fast-growing crop for biofuels and chemicals production, Biofuels, Bioproducts and Biorefining, 6, 580-598, 10.1002/bbb.1353, 2012.

Erbs, M., Manderscheid, R., Jansen, G., Seddig, S., Pacholski, A., and Weigel, H.-J.: Effects of free-air CO2 enrichment and nitrogen supply on grain quality parameters and elemental composition of wheat and barley grown in a crop rotation, Agriculture, Ecosystems & Environment, 136, 59-68, 10.1016/j.agee.2009.11.009, 2010.

Fageria, N. K.: Growth and mineral nutrition of field crops, Books in soils, plants, and the environment, edited by: Baligar, V. C., and Jones, C. A., Dekker, New York u.a., 1991.

FAOSTAT: Crops (National Production): http://www.fao.org/data/en/, access: 2017-31-05, 2017.

Hartmann, J., and Moosdorf, N.: Chemical weathering rates of silicate-dominated lithological classes and associated liberation rates of phosphorus on the Japanese Archipelago—Implications for global scale analysis, Chemical Geology, 287, 125-157, 10.1016/j.chemgeo.2010.12.004, 2011.

Hartmann, J., West, A. J., Renforth, P., Köhler, P., De La Rocha, C. L., Wolf-Gladrow, D. A., Dürr, H. H., and Scheffran, J.: Enhanced chemical weathering as a geoengineering strategy to reduce atmospheric carbon dioxide, supply nutrients, and mitigate ocean acidification, Rev Geophys, 51, 113-149, 10.1002/Rog.20004, 2013.

Hartmann, J., Moosdorf, N., Lauerwald, R., Hinderer, M., and West, A. J.: Global chemical weathering and associated P-release — The role of lithology, temperature and soil properties, Chemical Geology, 363, 145-163, 10.1016/j.chemgeo.2013.10.025, 2014.

Jasinski, M.: Minerals Yearbook: Volume I.-- Metals and Minerals, U.S. Geological Survey, 2017.

Maher, K.: The role of fluid residence time and topographic scales in determining chemical fluxes from landscapes, Earth and Planetary Science Letters, 312, 48-58, 10.1016/j.epsl.2011.09.040, 2011.

Manning, D. A. C.: How will minerals feed the world in 2050?, Proceedings of the Geologists' Association, 126, 14-17, 10.1016/j.pgeola.2014.12.005, 2015.

Moosdorf, N., Renforth, P., and Hartmann, J.: Carbon dioxide efficiency of terrestrial enhanced weathering, Environ Sci Technol, 48, 4809-4816, 10.1021/es4052022, 2014.

Renforth, P., Jenkins, B. G., and Kruger, T.: Engineering challenges of ocean liming, Energy, 60, 442-452, 10.1016/j.energy.2013.08.006, 2013.

Schopka, H. H., Derry, L. A., and Arcilla, C. A.: Chemical weathering, river geochemistry and atmospheric carbon fluxes from volcanic and ultramafic regions on Luzon Island, the Philippines, Geochim Cosmochim Ac, 75, 978-1002, 10.1016/j.gca.2010.11.014, 2011.